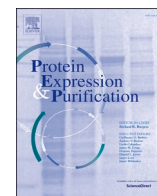




Contents lists available at ScienceDirect

Protein Expression and Purification

journal homepage: www.elsevier.com/locate/yprep

Recombinant production of antibody antigen-binding fragments with an N-terminal human growth hormone tag in mammalian cells

Yuriko Adachi^a, Mika K. Kaneko^b, Yukinari Kato^{b,c}, Terukazu Nogi^{a,*}^a Graduate School of Medical Life Science, Yokohama City University, 1-7-29 Suehiro-cho, Tsurumi-ku, Yokohama, 230-0045, Japan^b Department of Antibody Drug Development, Tohoku University Graduate School of Medicine, 2-1 Seiryomachi, Sendai, Miyagi, 980-8575, Japan^c Department of Molecular Pharmacology, Tohoku University Graduate School of Medicine, 2-1 Seiryomachi, Sendai, Miyagi, 980-8575, Japan

ARTICLE INFO

Keywords:

Monoclonal antibody
 Fab production
 Mammalian cell expression
 Human growth hormone
 Immobilized metal chelate affinity chromatography

ABSTRACT

Antigen-binding fragments (Fabs) of antibodies are both key biopharmaceuticals and valuable tools for basic life science. To streamline the production of diverse Fabs by capitalizing on standard and highly optimized protein production protocols, we here explore a method to prepare recombinant Fabs as secreted fusion proteins with an N-terminal human growth hormone domain and an octa-histidine tag. These tagged Fabs can be purified with standard immobilized metal chelate affinity chromatography. We first demonstrated Fab overproduction using the rat monoclonal antibody NZ-1. Optimization of linker residues enabled the complete removal of the tags by TEV protease, leaving only two additional residues at the N-terminus of the heavy chain. We purified NZ-1 Fab at ~4 µg/mL of culture supernatant and further confirmed that the NZ-1 Fab from the fusion protein maintained its native fold and binding affinity for target cell-surface antigens. We also showed that several other Fabs of mouse IgG₁s, the major subclass in mice, could be produced with the same procedure. Our preparation method can provide greater flexibility in functional and structural modifications of target Fabs because specialized purification techniques are not necessary.

1. Introduction

Antigen-binding fragments (Fabs) of monoclonal antibodies are beneficial in both medical and pharmaceutical sciences and in other fields such as molecular and cellular biology. Notably, Fabs have facilitated structure determination of challenging targets in structural biology. For instance, Fabs serve as crystallization chaperones that promote packing formation of membrane proteins covered with fluidic detergent-micelles in X-ray crystallography [1,2]. Fabs have also been shown to enable single-particle cryo-EM analysis of low-molecular-weight proteins as fiducial markers for particle micrograph alignment [3,4]. However, applying Fabs to crystallization and cryo-EM analyses demands their production in milligram or sub-milligram quantities. There have been two major strategies employed in the preparation of Fabs: digestion of full-length antibodies and recombinant production of partial fragments [5]. Fabs are composed of the variable heavy (VH), constant heavy 1 (CH1), variable light (VL), and constant light (CL) regions, and can be prepared by cleaving the hinge region between CH1 and constant heavy 2 (CH2) with papain. However, the digestion of IgG or IgM requires optimized

reaction conditions and the separation of the post-cleavage fragments, frequently leading to lower yields. It is also possible to produce Fabs recombinantly using cDNA in both bacterial and mammalian expression systems, but the production levels in both systems will vary depending on the Fab sequence. Additionally, specialized techniques such as affinity purification with Protein L-immobilized resin are necessary to separate Fabs from crude extracts because Fabs lack the Fc region and do not bind Protein A. Further, the application of Protein L-immobilized resin is limited to the antibodies containing specific subtypes of the kappa light chain [6]. Antigen-conjugated resins can be used to purify Fabs, but these are not generalizable and not commercially available in most cases.

Thus, we explored an alternative method to prepare Fabs reproducibly by using conventional separation techniques. Specifically, we produced Fabs as secreted fusion proteins with N-terminal human growth hormone (hGH) and octa-histidine (His₈) tags using a pSGHV0 vector [7] in mammalian cells and to purified them by immobilized metal chelate affinity chromatography. In this expression system, the hGH and His₈ tags can be cleaved off specifically and efficiently by TEV protease after purification, leaving only a few residues derived from the

* Corresponding author.

E-mail address: nogi@yokohama-cu.ac.jp (T. Nogi).<https://doi.org/10.1016/j.pep.2023.106289>

Received 11 April 2023; Received in revised form 24 April 2023; Accepted 27 April 2023

Available online 7 May 2023

1046-5928/© 2023 Elsevier Inc. All rights reserved.

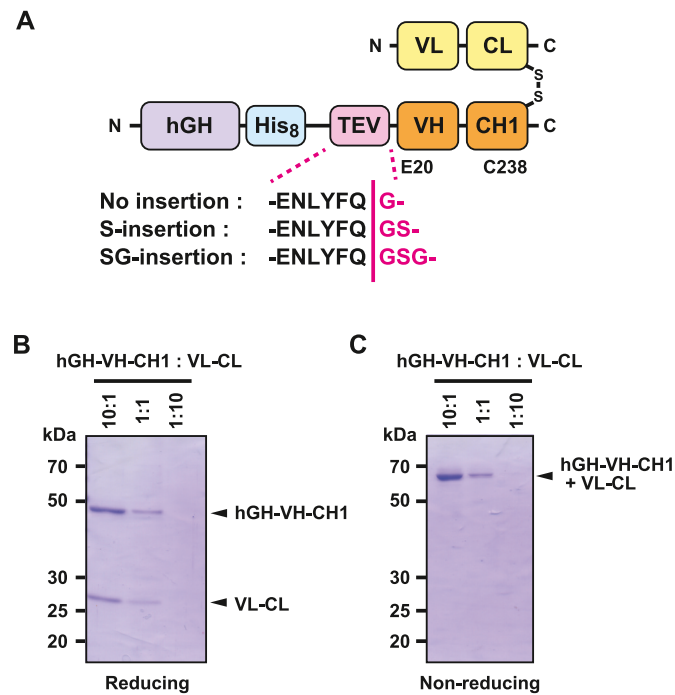


Fig. 1. Production of the NZ-1Fab as an hGH-fusion protein (A) Construct design. The hGH and His₈ tags and the TEV protease consensus sequence were fused to the N-terminus of the NZ-1 VH-CH1 region comprised of heavy chain residues E20 to C238. In NZ-1 (rat IgG_{2a}), C238 forms a disulfide bond with the Cys residue at the C-terminus of the light chain. The TEV protease consensus sequence was directly connected to E20 on the VH region in the initial construct while the Ser and Ser-Gly residues were inserted after the Gly residue of the consensus sequence in the modified constructs. (B, C) Small-scale production of the hGH-fused NZ-1 Fab with no insertion. The hGH-fused NZ-1 Fabs purified from the culture supernatant with Ni-NTA agarose were separated by SDS-PAGE under reducing (B) and non-reducing (C) conditions. The plasmids encoding the hGH-VH-CH1 and VL-CL regions were mixed at mass ratio indicated above the gel image.

recognition sequence at the N-terminus. We first produced an Fab for the rat monoclonal antibody NZ-1 (IgG_{2a}, lambda) [8] to demonstrate the feasibility of the hGH-fusion strategy. The NZ-1 antibody has been utilized in a variety of applications ranging from medical science to biochemistry. NZ-1 recognizes 14 residues of human podoplanin (PA14) expressed on cancer cells, and it suppress the platelet aggregation by inhibiting the binding of CLEC-2 to podoplanin [9]. As NZ-1 shows an extremely high affinity to the 12 C-terminal residues (PA12) of PA14, the PA12/NZ-1 pair has been developed as an immunoaffinity purification system [10]. Furthermore, NZ-1 forms stable complexes with PA12- or PA14-grafted target proteins [11,12], raising possibilities that the NZ-1 Fab can serve as crystallization chaperone or fiducial markers in structural analysis. After examining the structure and function of the NZ-1 Fab produced as the hGH-fusion protein, we also demonstrated the broad applicability of our hGH-fusion strategy by producing several mouse monoclonal antibodies belonging to IgG₁, the major subclass for mouse IgG.

2. Results and discussion

2.1. Production of hGH-fused fab

We produced the heavy chain fragment as a hGH-fusion protein (Fig. 1A), which mediates secretion of the recombinant fusion protein. The cDNA encoding residues 20 to 238 of the NZ-1 heavy chain (corresponds to the VH-CH1 regions) was cloned into the pSGHV0 secretion expression vector. The constructed plasmid was then transfected into mammalian cells (Expi293F) together with a plasmid encoding the cDNA of the NZ-1 light chain. When the culture supernatant was applied to Ni-NTA agarose, a disulfide-linked complex of the hGH-VH-CH1 and VL-CL segments appeared in the elution fraction as confirmed by SDS-PAGE. Furthermore, the expression level of the complex increased when the plasmids for the heavy and light chains were mixed at a mass

ratio of 10:1 in the transfection (Fig. 1B and C). Subsequently, we attempted to remove the hGH-His₈ portion by adding TEV protease to the elution fraction. However, majority of hGH-VH-CH1 remained uncleaved (Fig. 2A, D). In this construct, the TEV protease consensus sequence was directly fused to the N-terminal residue of VH (Glu-20) (Fig. 1A). Thus, we inferred that the steric hindrance between TEV protease and VH reduced the cleavage efficiency.

2.2. Optimization of TEV cleavable linker for efficient removal of the N-terminal tags

We next modified the fusion protein to eliminate steric hindrance for TEV protease. TEV protease cleaves between Gln and Gly in the consensus sequence (ENLYFQG). We inserted linker residues, Ser or Ser-Gly, after the Gly residue in the consensus sequence (Fig. 1A). The cleavage efficiency was greatly improved for the two resulting insertion mutations such that the vast majority of both were cleaved by TEV protease (Fig. 2B,C,E,F) under the previous reaction conditions. We therefore worked to establish a purification protocol for Fabs using the construct with the more minimal single Ser insertion (hereafter, the hGH-fused Fab is referred to as hGH-GS-Fab and the post-cleavage product is referred to as GS-Fab). After the tag cleavage, hGH-His₈ and His-tagged TEV protease were removed using Ni-NTA agarose resin. Finally, gel filtration was performed to collect the GS-Fab in a mono-disperse state (Fig. 3A and B).

2.3. Flow cytometry to examine the binding affinity to cell surface antigens

We subsequently examined if the recombinant NZ-1 GS-Fab maintained its function. NZ-1 was originally established as a highly reactive antibody against human podoplanin and was used to suppress podoplanin-induced platelet aggregation. It has also been reported that

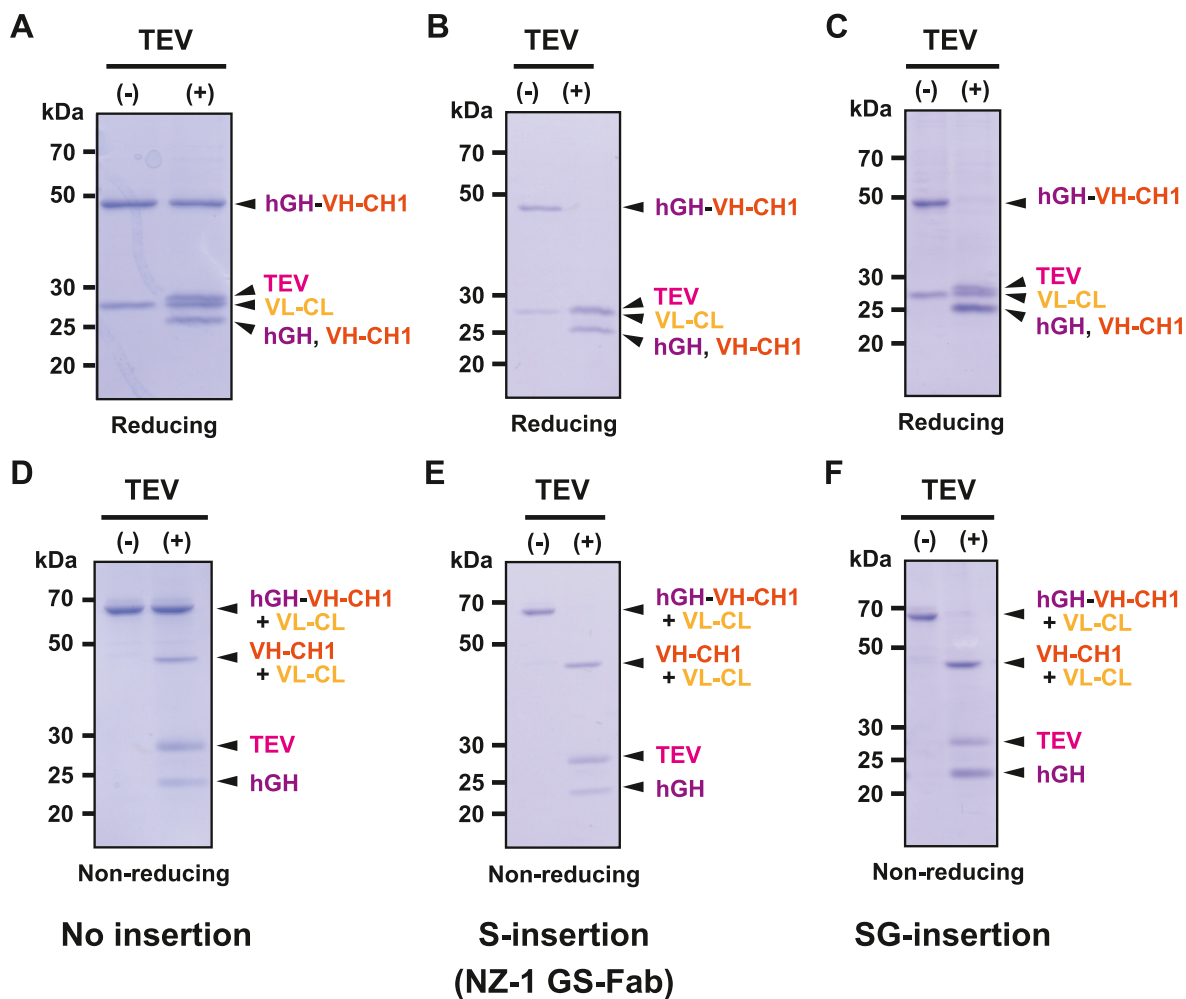


Fig. 2. Cleavage of the N-terminal tags by TEV protease. (A, D) The initial construct with no insertion. (B, E) The modified construct with the single Ser insertion (NZ-1 GS-Fab). (C, F) The modified construct with the Ser-Gly insertion. The hGH-fused NZ-1 Fab samples before (-) and after (+) cleavage were separated by SDS-PAGE under reducing (A–C) and non-reducing (D–F) conditions. The bands for the hGH and the VH-CH1 fragments generated by the cleavage appeared to overlap under reducing conditions.

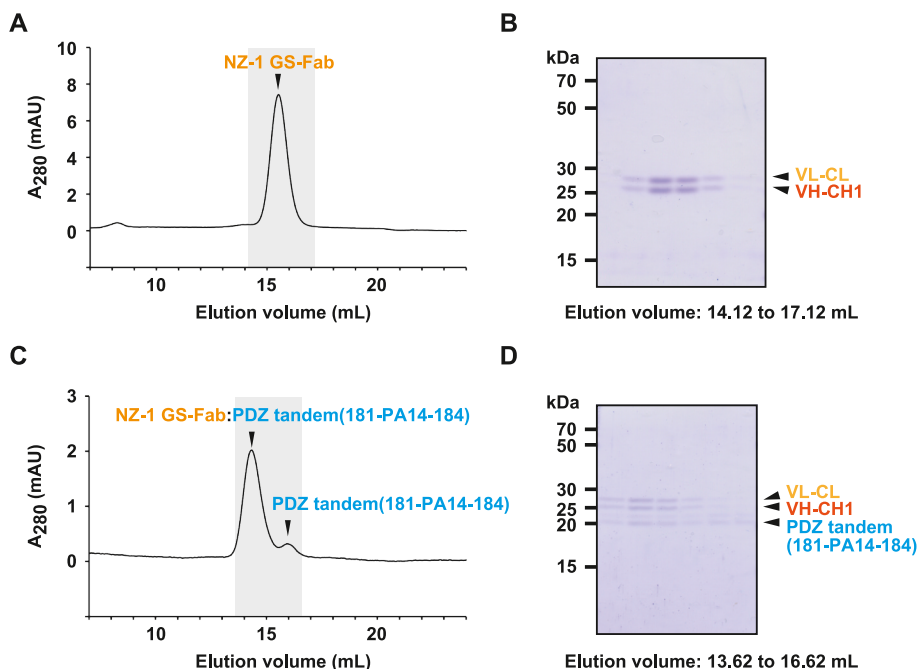


Fig. 3. Analytical gel filtration of the NZ-1 GS-Fab. (A) The monodisperse peak of the NZ-1 GS-Fab appeared in the elution from gel filtration. The six fractions around the peak (grey background) were separated by SDS-PAGE under reducing conditions in (B). (C) When mixed with PDZ tandem(181-PA14-184), the peak shifted to the higher molecular weight side while a peak of residual PDZ tandem was also observed. The six fractions containing the complex and the residual PDZ tandem (grey background) were separated by SDS-PAGE under reducing conditions in (D).

NZ-1 strongly bound with human podoplanin expressed on CHO cells. We therefore performed flow cytometry on podoplanin-expressing CHO (CHO/hPDPN) cells to compare the binding affinities between the NZ-1 GS-Fab and the IgG-digested NZ-1 Fab. We applied serial two-fold dilution of GS-Fab or IgG-digested Fab ranging from 10 to 0.0006 $\mu\text{g}/\text{mL}$, which corresponds to 240 to 0.013 nM, to the CHO/hPDPN cells. Binding data were fit to a sigmoidal 2-state binding model, and the dissociation constants for GS-Fab and IgG-digested Fab were estimated at 2.37 and 5.19 nM, respectively (Fig. 4). It is therefore presumed that the complementarity determining regions were properly formed in the NZ-1 GS-Fab produced as a hGH-fusion protein despite the difference of expression method and the presence of the additional Gly-Ser residues at the N-terminus as compared to the IgG-digested NZ-1 Fab.

2.4. Structural analysis to verify the folding of GS-Fab

To test if the entire NZ-1 GS-Fab maintains its native folding and disulfide bonding pattern, we also performed X-ray crystallographic analysis on the complex with a PA14-grafted protein. In a previous study, we demonstrated that the PA14 sequence can be inserted into β -hairpin regions in the periplasmic domain of an intramembrane protease, the PDZ tandem fragment of the RseP orthologue from the hyperthermophile *Aquifex aeolicus*. We also crystallized the complex of the IgG-digested NZ-1 Fab and the PA14-grafted protease extracellular domain, termed PDZ tandem(181-PA14-184), in which PA14 is inserted between Arg-181 and Glu-184 [12]. In this study, we performed analytical gel filtration to examine if the above purified NZ-1 GS-Fab forms a stable complex with PDZ tandem(181-PA14-184). The elution peak for NZ-1 GS-Fab was indeed shifted to the higher molecular weight side when mixed with PDZ tandem(181-PA14-184). The complex eluted in a monodisperse state with no apparent dissociation, indicating that GS-Fab was tightly bound to the PA14-grafted PDZ tandem (Fig. 3C and D). Subsequently, we purified approximately 1 mg of NZ-1 GS-Fab from a 240 mL culture of Expi293F cells to prepare the complex in larger quantities. Yields of IgGs prepared from the hybridoma vary widely, but typically fall in the range of 10–100 $\mu\text{g}/\text{mL}$ of culture supernatant.

Considering that the recovery of Fab from IgG after the papain digestion is only about 20% in some cases, the yield of NZ-1 GS-Fab ($\sim 4 \mu\text{g}/\text{mL}$ of culture supernatant) would be comparable to that of IgG-digested NZ-1 Fab.

NZ-1 GS-Fab complexed with PDZ tandem(181-PA14-184) produced crystals that diffracted X-ray to 2.2 \AA resolution. The crystal structure was solved by molecular replacement method using the atomic coordinates of the IgG-digested NZ-1 Fab complexed with PDZ tandem(181-PA14-814) as a search model (Table 1). The atomic models were almost identical between the two complexes where the 426 C α atoms in the Fabs were superposed onto one another with RMSD = 0.247 \AA (Fig. 5A–C). The Gly-Ser residues left on the N-terminus of the heavy chain after tag cleavage were far removed from the antigen-binding pocket and not involved in the interaction with PDZ tandem(181-PA14-184). The second Ser residue was clearly observed in the electron density map while the model for the first Gly residue was not assigned in the crystal structure due to disorder (Fig. 5D). These results confirmed that the NZ-1 GS-Fab prepared from the hGH-fusion protein adopted the quaternary structure equivalent to the Fab derived from the intact IgG.

2.5. Examination of the generalizability of the hGH-fusion method

Lastly, we attempted to overproduce Fabs that differ from NZ-1, a rat IgG_{2a} with a lambda light chain. We selected Fabs from mouse IgG_{1s} with kappa light chains: LpMab-7 against human podoplanin, 8B8 against the PDZ tandem fragment of RseP orthologue from *A. aeolicus*, 13F1 against the PDZ tandem fragment of RseP from *E. coli*. As with the NZ-1 GS-Fab, the hGH-His₆ tag was fused to the N-terminus of the heavy chain with the single Ser insertion between the TEV protease consensus sequence and the VH region for each of these four Fabs. All tested Fab constructs were successfully produced in mammalian cells, and as anticipated, the tags were digested almost completely after affinity purification (Fig. 6) without additional protocol optimization. These results support the applicability of the hGH-fusion method constructed in this study.

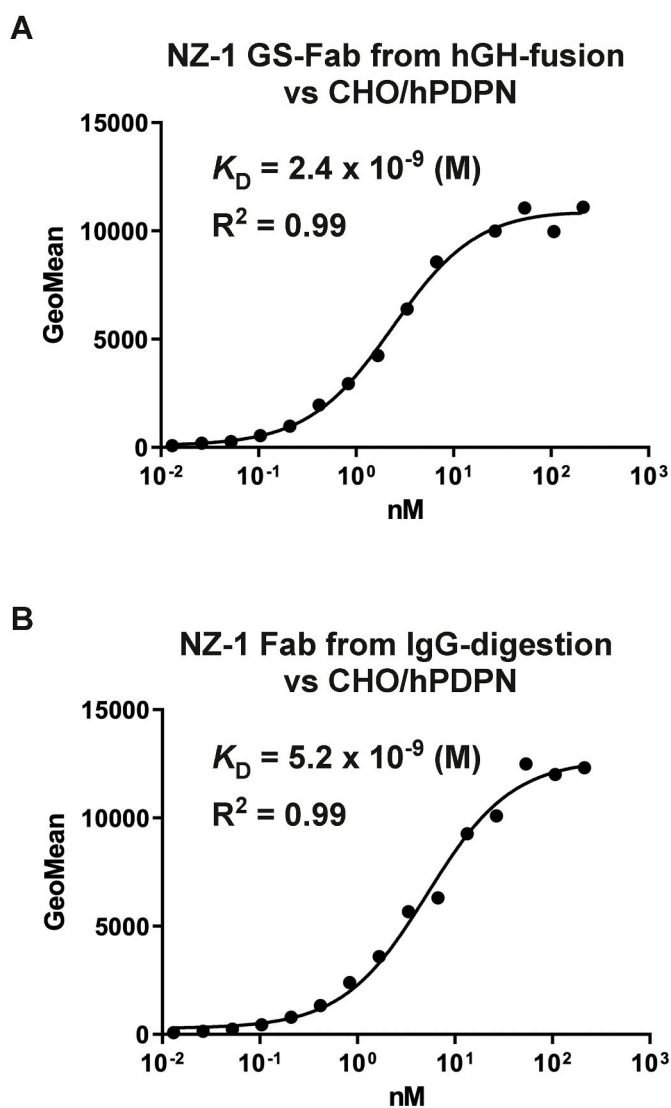


Fig. 4. Estimation of binding affinities of NZ-1 Fabs by flow cytometry. CHO/hPDPN cells were resuspended at 100 μ l of serially diluted NZ-1 GS-Fab produced as the hGH-fusion protein in (A) or NZ-1 Fab prepared by the IgG digestion in (B). K_D was calculated by fitting the binding isotherms of geometric mean of fluorescence intensities.

3. Conclusion

In this study, we have established an overproduction method for Fabs as hGH-fusion proteins. This method simplifies Fab purification, replacing specialized affinity resins with resins for conventional metal chelating affinity chromatography. The only structural difference between the Fabs prepared from the hGH-fusion and from the papain digestion of intact antibodies is the presence and absence of two residues (Gly-Ser) at the N-terminus of the heavy chain, which are expected to have little impact on the functions such as antigen recognition and neutralizing activity. Consistent with this expectation, the NZ-1 Fab prepared by the hGH-fusion was successfully crystallized in complex with an epitope-grated protein while it maintained its binding affinity for cell-surface antigens. Successful overproduction of Fabs from

Table 1
Statistics for X-ray crystallographic analysis.

Data Collection	
Space group	$P2_12_12_1$
Cell dimensions	
a, b, c (\AA)	51.94, 75.09, 173.52
α, β, γ ($^\circ$)	90, 90, 90
No. of complex/a.s.u.	1
X-ray source	PF/BL-17A
Wavelength (\AA)	0.9800
Resolution limits (\AA)	45.82–2.20 (2.27–2.20)
No. of unique reflection	35,390 (3,029)
Completeness (%)	100 (100)
Redundancy	6.7 (6.9)
$\langle I/\sigma(I) \rangle$	16.7 (1.7)
R_{merge}^a	0.076 (1.205)
CC (1/2)	0.999 (0.738)
Refinement	
Resolution limits (\AA)	38.32–2.20 (2.23–2.20)
R_{work}^b	0.2427 (0.3500)
R_{free}^c	0.2698 (0.3562)
No. of non-H atoms	4,802
Average B -factor (\AA^2)	62.38
RMSD from ideality	
Bond length (\AA)/angle ($^\circ$)	0.002/0.54
Ramachandran plot	
Favored/Outlier (%)	95.51/0.50
PDB code	8IPC

Values in parentheses are for highest-resolution shell.

^a $R_{\text{merge}} = \sum_h \sum_i |I_i(h) - \langle I(h) \rangle| / \sum_h \sum_i I_i(h)$, where $I_i(h)$ is the i th measurement.

^b R_{work} is the crystallographic R -factor (R_{cryst}) for the working set used for the refinement. $R_{\text{cryst}} = \sum_h ||F_{\text{obs}}(h)| - |F_{\text{calc}}(h)|| / \sum_h |F_{\text{obs}}(h)|$, where $F_{\text{obs}}(h)$ and $F_{\text{calc}}(h)$ are the observed and calculated structure factors.

^c R_{free} is R_{cryst} calculated for the test set consisting of 5% of reflections excluded from the refinement.

unrelated mouse monoclonal antibodies without the need for additional protocol optimization demonstrates the generalizability of this method. Because specialized purification techniques and re-optimized tag cleavage conditions were not necessary, this method will provide greater flexibility in functional and structural modifications of target Fabs.

CRedit author statement

Yuriko Adachi: Investigation, Writing – original draft.

Mika K. Kaneko: Investigation.

Yukinari Kato: Investigation, Funding acquisition, Supervision, Writing – original draft, Writing – review & editing.

Terukazu Nogi: Conceptualization, Investigation, Funding acquisition, Project administration, Writing – original draft, Writing – review & editing.

Declaration of competing interest

The corresponding author declares no financial and non-financial competing interests on behalf of all authors.

Data availability

Data will be made available on request.

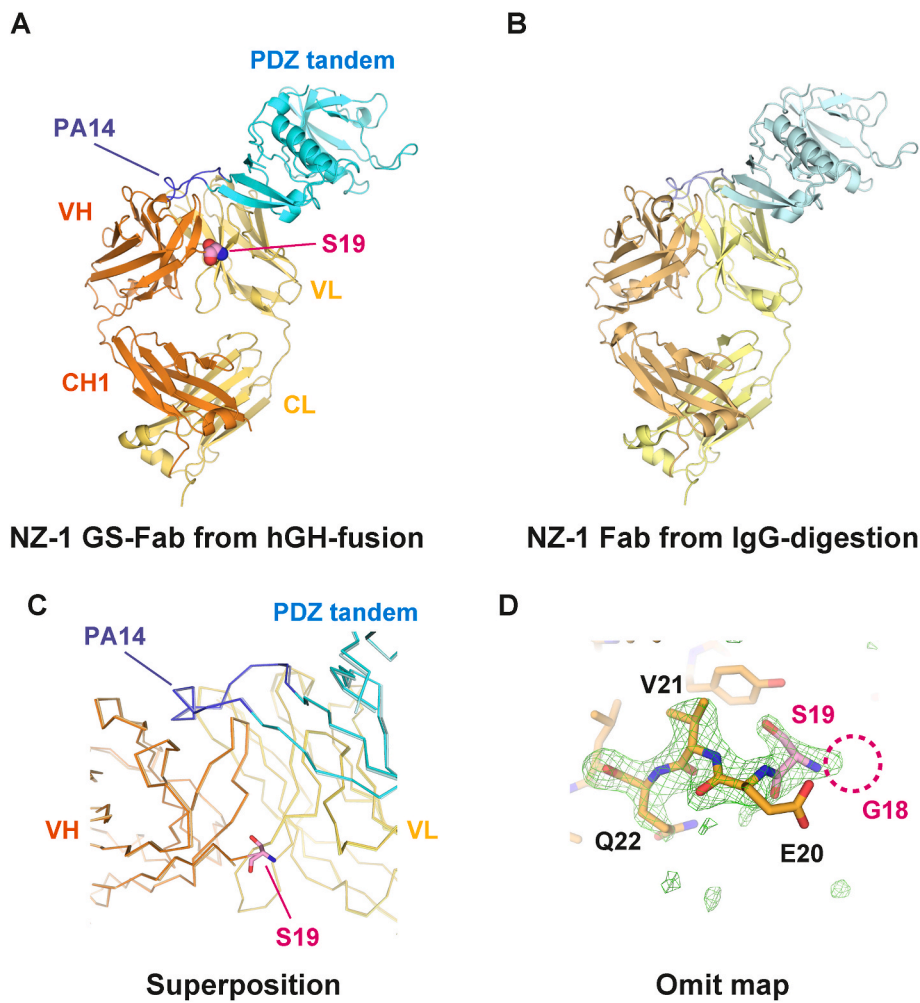


Fig. 5. Crystallographic analysis of the NZ-1 GS-Fab. (A) Crystal structure of the NZ-1 GS-Fab in complex with PDZ tandem(181-PA14-184). The grafted PA14 epitope was colored blue. The Ser residue inserted between the TEV protease consensus sequence and the VH region was depicted with spheres and labeled S19. (B) Crystal structure of the IgG-digested NZ-1 Fab in complex with PDZ tandem(181-PA14-184). The previously determined structure (PDB code: 7CQC) is shown in the same view as in (A). (C) Superposition of the two complexes. The C α traces of the two complexes are shown in the same colors as in (A) and (B). (D) Omit map around the N-terminus of the heavy chain. The mFo-DFc map (green mesh) was calculated by omitting the atomic coordinates of the residues S19-Q22 from the final model. Atomic coordinates S19 could be fit to the map, but no obvious electron density was observed for Gly18. The putative position of Gly18 is indicated by a magenta dotted circle.

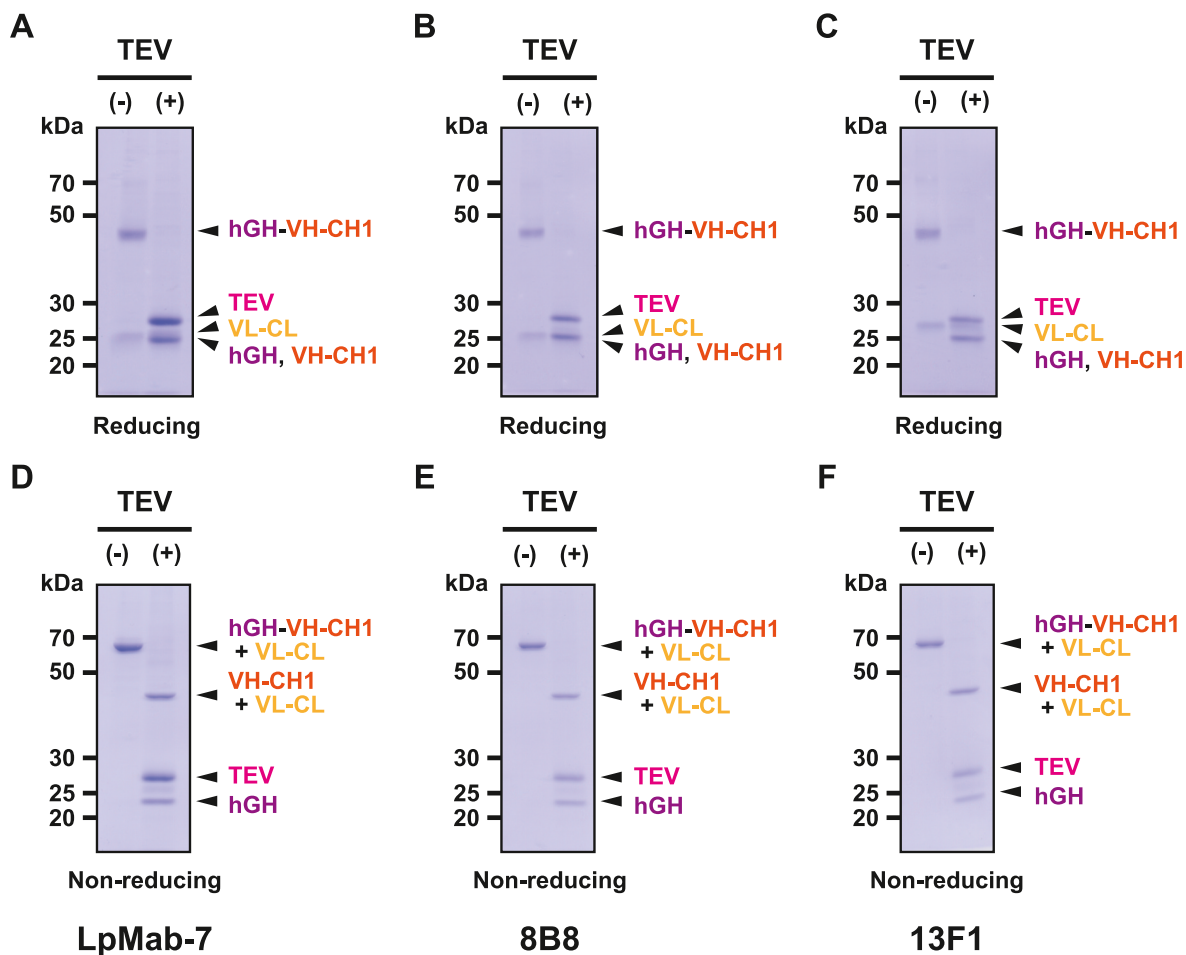


Fig. 6. Production of Fabs from mouse IgG₁s as hGH-fusion proteins (A, D) LpMab-7. (B, E) 8B8. (C, F) 13F1. The hGH-fused mouse IgG₁ Fab samples before (-) and after (+) cleavage were separated by SDS-PAGE under reducing (A–C) and non-reducing (D–F) conditions.

Acknowledgements

We are grateful to the beamline staff of Photon Factory (Tsukuba, Japan) for providing data collection facilities and support. We thank Samuel Thomson for editing the manuscript, and associate profs. Norimichi Nomura and Satoshi Ogasawara, and prof. Taro Tamada for valuable discussions and information on Fab preparation. This research was partially supported by the Japan Society for the Promotion of Science (JSPS) KAKENHI under Grant Numbers JP22H02561, and JP19H03170 (to T.N.), by Japan Agency for Medical Research and Development (AMED) under Grant Number: JP22ama121008 (to Y.K.), by the Cooperative Research Program (Joint Usage/Research Center program) of Institute for Life and Medical Sciences, Kyoto University (to T.N.), and by the Cooperative Research Project Program of Life Science Center for Survival Dynamics, Tsukuba Advanced Research Alliance (TARA Center), University of Tsukuba (to T.N.). This work was performed partially under the Collaborative Research Program of Institute for Protein Research, Osaka University, CR-21-01.

Material and Methods

Antibodies and expression plasmids

NZ-1 was generated by immunizing rats with 14 amino acids from residue 38 to residue 51 of human podoplanin [8]. LpMab-7 was generated by immunizing mice with human podoplanin-overexpressed LN229 glioblastoma cells [13]. 8B8 and 13F1 were generated by immunizing GANP mice [14] with a mixture of PDZ tandem fragments of *E. coli* RseP and its orthologue from *Aquifex aeolicus* as reported previously [15]. 8B8 was selected as a monoclonal antibody against the PDZ tandem from *A. aeolicus* RseP while 13F1 was selected against the PDZ tandem from *E. coli* RseP. For the heavy chain of NZ-1, cDNA for the VH-CH1 region was subcloned between the BamHI and EcoRI sites in the pSGHV0 vector using the In-Fusion HD Cloning Kit (Takara Bio). The Ser or Ser-Gly insertions between the TEV protease consensus sequence and the NZ-1 VH region were introduced by the inverse PCR method. For the heavy chains of LpMab-7, 8B8, and 13F1, cDNAs encoding the VH-CH1 region were amplified with primers that added an additional Ser residue at the N-terminus. These cDNAs were then subcloned into the pSGHV0 vector [7]. The cDNAs encoding the light chains with the original signal sequences were subcloned into the pCAG-Neo vector (FUJIFILM Wako Pure Chemical Corporation, Osaka, Japan).

Protein expression and purification

Expression plasmids for the heavy and light chains were mixed at mass ratios of 10:1, 1:1, or 1:10 and transfected into Expi293F™ cells (Thermo Fisher Scientific) using the ExpiFectamine™ 293 Transfection Kit (Thermo Fisher Scientific). The cells were cultured in 2 mL medium in a 6-well plate, or 30 mL medium in a 125-mL flask. Larger production batches used multiple 30 mL cultures. After pelleting the cells by centrifugation, the culture supernatant was neutralized by adding Tris-Cl (pH8.0) at a final concentration of 20 mM for efficient target protein binding to Ni-NTA agarose resin (QIAGEN). After incubating with the culture supernatant, the resin was washed with 20 mM Tris-Cl (pH 8.0), 300 mM NaCl, and 10 mM imidazole. Subsequently, the captured proteins were eluted with 20 mM Tris-Cl (pH8.0), 300 mM NaCl, and 250 mM imidazole. N-terminally hexahistidine-tagged TEV protease (His₆-TEV) was added to the elution fraction to cleave off the N-terminal hGH and His₈ tags. For further purification, the cleavage fraction was dialyzed against 10 mM Tris-Cl (pH 8.0), and 150 mM NaCl overnight at 4 °C using the dialysis membrane with molecular weight cut-off of 3,500. The cleaved hGH-His₈ portion and His₆-TEV were removed by passing the fraction through Ni-NTA agarose resin. Finally, the flow-through and wash fractions containing Fabs were further purified by gel filtration on a Superdex™ 200 Increase 10/300 GL (Cytiva) column

equilibrated in 10 mM Tris-Cl (pH 7.4), and 150 mM NaCl. The peak fractions containing target proteins were concentrated by ultrafiltration using an Amicon® Ultra Centrifugal Filter with a molecular weight cut-off of 30 kDa (Merck Millipore).

Determination of binding affinities by flow cytometry

Serially diluted antibodies (10 µg/ml - 0.6 ng/ml) were treated with CHO/hPDPN cells. The cells were further incubated with Alexa Fluor 488-conjugated anti-rat IgG (1:200; Cell Signaling Technology, Inc., Danvers, MA, USA). Fluorescence data were collected using a BD FACSLyric flow cytometer and analyzed using BD FACSuite software version 1.3 (BD Biosciences, Franklin Lakes, NJ, USA). The K_D values were determined by GraphPad Prism 8 (the fitting binding isotherms to built-in one-site binding models; GraphPad Software, Inc., La Jolla, CA, USA).

X-ray crystallographic analysis

The PA14-grafted PDZ tandem fragment, PDZ tandem(181-PA14-184), was produced as an N-terminal GST-fusion protein in *E. coli* BL21(DE3) cells. The purification procedure was essentially the same as reported previously [12]. The purified PDZ tandem(181-PA14-184) was mixed with NZ-1 GS-Fab and applied to a Superdex™ 200 Increase 10/300 GL SEC column (Cytiva) equilibrated with 10 mM Tris-Cl (pH 7.4), and 150 mM NaCl to fractionate the complex.

Initial crystallization conditions were searched using the Index™ (Hampton Research) screening kit. 0.2 µL each of protein solution and crystallization buffer were dispensed into 96-well plates using a Crystal Gryphon (Art Robbins Instruments) and equilibrated against 60 µL of crystallization buffer in the reservoir by the sitting-drop vapor-diffusion method. After optimization, PDZ tandem(181-PA14-184) complexed with the NZ-1 GS-Fab was crystallized in a solution containing 14% (wt./vol.) polyethylene glycol 3,350, 0.2 M lithium sulfate, and 0.1 M Bis-Tris-HCl (pH 6.5).

Crystals were flash frozen in liquid nitrogen after being quickly soaked in cryoprotectant, which was prepared by mixing the crystallization buffer and ethylene glycol in a ratio of 4:1 (vol/vol). X-ray diffraction data were collected using PILATUS3 S 6 M (Dectris) at Photon Factory (PF) BL-17A (Tsukuba, Japan). Data were processed and scaled with XDS [16] and aimless [17]. Diffraction intensities were subsequently converted to structure factors using the CCP4 suite [18] where 5% of the unique reflections were randomly selected for the calculation of free R-factor.

Initial phases were determined by the molecular replacement method using Molrep [19], in which the crystal structure of the PDZ tandem(181-PA14-184) complexed with IgG-digested NZ-1 Fab was used as a search model. The initial model was manually modified and fit into the electron density map using the program COOT [20]. The updated models were refined with phenix.refine [21] iteratively while monitoring the stereochemistry with MolProbity [22]. Statistics for X-ray crystallographic analysis are summarized in Table 1. Structural superposition and RMSD calculation were performed by a pair-wise alignment protocol using LSQKAB [23]. Figures for protein structures were prepared with PyMOL (The PyMOL Molecular Graphics System, Version 2.3 Schrödinger, LLC.).

The atomic coordinates and structure factors of PDZ tandem(181-PA14-184) complexed with NZ-1 GS-Fab have been deposited in the Protein Data Bank with an accession number of 8IPC.

References

- [1] T. Hino, S. Iwata, T. Murata, Generation of functional antibodies for mammalian membrane protein crystallography, *Curr. Opin. Struct. Biol.* 23 (2013) 563–568.
- [2] C. Hunte, H. Michel, Crystallisation of membrane proteins mediated by antibody fragments, *Curr. Opin. Struct. Biol.* 12 (2002) 503–508.
- [3] R. Nygaard, J. Kim, F. Mancina, Cryo-electron microscopy analysis of small membrane proteins, *Curr. Opin. Struct. Biol.* 64 (2020) 26–33.

- [4] S. Wu, et al., Fabs enable single particle cryoEM studies of small proteins, *Structure* 20 (2012) 582–592.
- [5] Y. Zhao, et al., Two routes for production and purification of Fab fragments in biopharmaceutical discovery research: papain digestion of mAb and transient expression in mammalian cells, *Protein Expr. Purif.* 67 (2009) 182–189.
- [6] B.H. Nilson, A. Solomon, L. Bjorck, B. Akerstrom, Protein L from *Peptostreptococcus magnus* binds to the kappa light chain variable domain, *J. Biol. Chem.* 267 (1992) 2234–2239.
- [7] D.J. Leahy, C.E. Dann 3rd, P. Longo, B. Perman, K.X. Ramyar, A mammalian expression vector for expression and purification of secreted proteins for structural studies, *Protein Expr. Purif.* 20 (2000) 500–506.
- [8] Y. Kato, et al., Inhibition of tumor cell-induced platelet aggregation using a novel anti-podoplanin antibody reacting with its platelet-aggregation-stimulating domain, *Biochem. Biophys. Res. Commun.* 349 (2006) 1301–1307.
- [9] S. Ogasawara, M.K. Kaneko, J.E. Price, Y. Kato, Characterization of anti-podoplanin monoclonal antibodies: critical epitopes for neutralizing the interaction between podoplanin and CLEC-2, *Hybridoma* 27 (2008) 259–267.
- [10] Y. Fujii, et al., PA tag: a versatile protein tagging system using a super high affinity antibody against a dodecapeptide derived from human podoplanin, *Protein Expr. Purif.* 95 (2014) 240–247.
- [11] R. Tamura, et al., Application of the NZ-1 Fab as a crystallization chaperone for PA tag-inserted target proteins, *Protein Sci.* 28 (2019) 823–836.
- [12] R. Tamura-Sakaguchi, et al., Moving toward generalizable NZ-1 labeling for 3D structure determination with optimized epitope-tag insertion, *Acta Crystallogr. D* 77 (2021) 645–662.
- [13] Y. Kato, M.K. Kaneko, A cancer-specific monoclonal antibody recognizes the aberrantly glycosylated podoplanin, *Sci. Rep.* 4 (2014) 5924.
- [14] N. Sakaguchi, et al., Generation of high-affinity antibody against T cell-dependent antigen in the Ganp gene-transgenic mouse, *J. Immunol.* 174 (2005) 4485–4494.
- [15] Y. Hizukuri, et al., A structure-based model of substrate discrimination by a noncanonical PDZ tandem in the intramembrane-cleaving protease RseP, *Structure* 22 (2014) 326–336.
- [16] W. Kabsch, XDS, *Acta Crystallogr. D* 66 (2010) 125–132.
- [17] P.R. Evans, G.N. Murshudov, How good are my data and what is the resolution? *Acta Crystallogr. D* 69 (2013) 1204–1214.
- [18] M.D. Winn, et al., Overview of the CCP4 suite and current developments, *Acta Crystallogr. D* 67 (2011) 235–242.
- [19] A. Vagin, A. Teplyakov, MOLREP: an automated program for molecular replacement, *J. Appl. Crystallogr.* 30 (1997) 1022–1025.
- [20] P. Emsley, B. Lohkamp, W.G. Scott, K. Cowtan, Features and development of Coot, *Acta Crystallogr. D* 66 (2010) 486–501.
- [21] P.V. Afonine, et al., Towards automated crystallographic structure refinement with phenix.refine, *Acta Crystallogr. D* 68 (2012) 352–367.
- [22] V.B. Chen, et al., MolProbity: all-atom structure validation for macromolecular crystallography, *Acta Crystallogr. D* 66 (2010) 12–21.
- [23] W. Kabsch, A solution for the best rotation to relate two sets of vectors, *Acta Crystallogr. A* 32 (1976) 922–923.